Indian Journal of Chemistry
Vol. 60A, September 2021, pp. 1192-1200

Fluorine and chlorine gas storage by confinement inside boron nitrogen nanotubes

Yasmine Fatima Zohra Assas[a], Yamina Belmiloud[a,]*, Mohammed Lamine Abdelatif[a], Soraya Abtouche[a], Meziane Brahimi[a] & Bahoueddine Tangour[b]

[a]Laboratoire de Physico-Chimie Théorique et de Chimie Informatique(LPCTCI), Faculté de Chimie, USTHB. BP32 El alia 16111. Alger. Algérie

[b]Research Unity on Modeling in Fundamental Sciences and Didactics, Team of Theoretical Chemistry and Reactivity, University de Tunis El Manar, Tunis, Tunisia

*E-mail: belmiloudy@yahoo.fr

Received 08 March 2021; revised and accepted 05 August 2021

DFT calculations using the WB97XD and CAM-B3LYP functional and the basis set 6-31G(d,p) have been performed to study the interaction between the X_2 (X=F or Cl) molecule and boron nitrogen nanotubes (BNNTs). Each molecule is confined within BNNTs with different dimensions in either parallel or perpendicular positions along the nanotube axis. The interaction between X_2 molecule and BNNT nanotube differed according to the extension of the confinement space and the molecular orientation. Unlike Cl_2, F_2 forms a very stable complex with (4,4) and (5,5) BNNTs. The van der Waals interactions of the X_2 molecule with the BNNT leads to charge transfer and a change in the charge distribution in the X_2 molecule, producing a new detectable infrared signal of the X-X bond stretch which is dependent on nanotube diameter.

Keywords: Boron nitrogen nanotubes, Storage of F_2, Storage of Cl_2, van der Waals interactions, DFT

Boron nitrogen nanotubes (BNNTs) were first theoretically predicted[1] in 1994 and subsequently synthesised[2] in 1995. BNNTs are semiconductors with unique physico-chemical properties, such as heat resistance, relative chemical inertia, and uniform electronic properties[3–5]. These nanotubes are also hydrophobic compounds with high resistance to oxidation and radiation absorption. Experimental and theoretical interest is focused on broadening the application of BNNTs[6–11] in several fields. They are used in numerous areas such as gas storage, chemical sensors,[12] organic gas and vapour detectors,[13] and nanovectors in drug administration[14]. This wide variety of application is due to the ability of BNNTs to trap molecules inside their cavities, which give them exceptional characteristics. The cavity of the nanotube and the various phenomena that can occur in the interior of these nanotubes have been studied in several experimental and theoretical studies on different molecules such as dihydrogen[15–18] and H_2O[19,20]. The existing research has shown that the properties of the confined molecules depend mainly on the size of the nanotube and are influenced by the type of used nanotube[17,18].

BNNTs are isostructural and isoelectronic to carbon nanotubes (CNTs). However, BNNT and CNT can have very different properties which originate from the fact that the carbon atoms in CNT are covalently linked whereas in the case of BNNT, B-N bonds have a significant ionic component. Compared to carbon nanotubes, BNNTs have better gas absorption capacities. Indeed, the absorption behaviour of CNTs is very dependent on its chirality and its structure[21–23], two properties which are very difficult to control experimentally[20], and which make the use of CNTs experimentally difficult to use as a gas container. Conversely, the presence of a wide band gap in BNNTs of about 5.5 eV[4,24] makes the electronic properties roughly independent on the structure and makes it possible to produce stable absorbents of gas.

Difluorine (F_2) is a simple diatomic entity, made up of two fluorine atoms. It is a light-yellow gas with an irritating odour, which is difficult to liquefy. F_2 is the most known powerful oxidizing agent, reacting with practically all organic or inorganic materials. This gas reacts violently and transforms on contact with moisture into hydrofluoric acid. It is also used in the synthesis of UF6 in the enrichment of uranium. Fluorine gas is corrosive to the respiratory tract and can penetrate deep into body tissue causing extremely damaging effects. In view of its risks, the storage and transport of F_2 gas constituted a great technological challenge. Teflon is the most used material. Fluorine can be stored in steel cylinders with passivated interior or in nickel cylinders. In the laboratory,

glassware can transport fluoride under anhydrous conditions and often under low pressure.

However, fluorine gas has very high reactivity and corrosivity, and very high technical capacity is required for its storage and handling. Alternative solutions have been proposed to store and produce fluorine through the synthesis of fluorinated compounds[25]. We cite the example of processes directly using gaseous fluorine generated by electrolysis or a molten fluorinated salts but unfortunately these processes cannot be used repeatedly. Fluorination processes for a carbon nanotubes and nanohorns[26–28] have been described. The production of F_2 is achieved by heating fluorinated carbon to temperatures of the order of 200 °C. An amount of fluorine storage per unit mass of fluorinated materials comes to about 52.9% by mass.

Similar to F_2, chlorine gas (Cl_2) is also a powerful oxidant that reacts easily with other materials. It is very toxic and leads to severe inhalation toxicity and is harmful to the environment.[29] The storage of difluorine and dichlorine gas requires special and delicate conditions. Diverse studies have examined the properties of CNTs as absorbents for these gases[30], and the process of adsorption on the surfaces of CNTs and boron nitrogen nanotubes[31,32], though less work has been done on F_2 confinement within CNTs[33]. To date, there are no documented theoretical or experimental studies of the confinement of F_2 or Cl_2 within BNNTs.

The fluorine storage properties of nanostructured carbon materials are provided by the two modes of fluorine adsorption which are chemisorption and physisorption with a van der Waals-type metastable interaction. In this context, we wanted in this work to test another mode which consists in the encapsulation of F_2 and Cl_2 molecules in BNNTs. The main goal of this work is to test the capacity of these molecules to be trapped in the hollow spaces of these nanosystems and to leave them at low temperature. Our approach is not associated with an experimental approach of using this storage process which a priori would lead to a low mass by mass percentage. It represents a prospective study and provides numerical values associated with monitoring the reaction and determining the characteristics of the involved species.

Therefore, the objectives of this work are summarised below. We inserted an X_2 molecule (X=F or Cl) in a position perpendicular or parallel to the axis of the BNNTs using density functional theory (DFT) and examine the confinement energy, X-X bond length, and vibrational frequencies of the studied systems. The first target is to understand the different quantum phenomena that can occur during chemical or physical absorption of these halides on the nanoscale within the BNNT. The second goal is to compare the behaviour of confined $F_2$with that of Cl_2 by considering the partial ionic nature of the B-N bond, which induces a dipolar moment between the nanotube and the confined molecule.

Materials and Methods

Computational Methods

In the first step of this work, we obtained the different armchair BNNT nanotubes dimensions (4,4), (5, 5), (6, 6), (7,7) and (8,8) using the TubeGen 3.4 program[34]. The diameters of these BNNTs range from 5.83 Å to 11.09 Å. These nanotubes have been formed by connecting three unit cells along the cylinder axis. The terminal atoms of boron and nitrogen have been hydrogenated to saturate their valence and to minimize the end effects. These BNNTs have the formule $B_{32}N_{32}H_{16}$, $B_{40}N_{40}H_{20}$, $B_{48}N_{48}H_{24}$, $B_{56}N_{56}H_{28}$, and $B_{64}N_{64}H_{31}$. For the optimization of our system structure, we used the theory of functional density using the WB97XD[35,36] and CAM-B3LYP.[37] These functional consider the dispersion forces. The Gaussian basis set used in this work is 6-31G(d,p). All calculations are performed using Gaussian 09 software[38]. Frequency calculations showed that all structures were stationary points. The various results given in the literature have shown that the orientation of the molecule confined within a nanotube affects the interaction between the molecule and the nanotube. For this purpose, two orientations of the X_2 molecule have been considered: perpendicular ($\perp$) and parallel (//) to the axis of the BNNT, as illustrated in the Fig. 1.

Results and Discussion

To test the stability of the X_2@BNNT complex (X= F or Cl) and to determine the local energy minimum, the X_2 molecule was confined within boron nitrogen nanotubes with (*n, n*) dimensions, with *n* ranging from 4 to 8. These complexes were designed using the DFT approach and using the functional correlation of the CAM-B3LYP and WB97XD exchanges with the 6-31G(d,p) basis set. The absence of imaginary frequencies in the vibrational spectra for each complex is evidence of their stability.

To compare the stability of two dihalogen molecules (F_2 and Cl_2) in BNNTs, we analysed the

differences in the confinement energy of the halides depending on the change in the diameter of the nanotubes. Focus was then placed on the effect of the diameter of the bond length and the intensity of the vibration of X-X bond (X=F or Cl). To obtain the corrected interaction energies using the counterpoise correction procedure, we have also calculated the basis set superposition error (BSSE) corrections[39,40].

Energy of confinement

The confinement energies were calculated using the following relation:

$$E_{conf}(X_2@BNNT) = E(X_2@BNNT) - [E(X_2) + E(BNNT)] \quad \ldots (1)$$

E(X₂@BNNT) is the total energy of X_2 molecule (X=F or Cl) confined in the nanotube. *E(BNNT)* and *E(X₂)* are the total energy of the single-walled BNNT and free X_2 molecules, respectively.

All the calculated confinement energies are listed in Table 1 and their variations are shown in Fig. 2. Analyses of these results show that the confinement energy is influenced by several parameters, such as the type of confined molecule (F_2 or Cl_2), the position of the X_2 molecule within the nanotube and the diameter of the nanotube. These observations are in perfect agreement with the reports on other molecules confined indifferent types of nanotubes.[16–18] The confinement energies calculated herein with the CAM-B3LYP and WB97XD functional were awfully close.

The results show that in both orientations, confinement of F_2 in the boron–nitrogen nanotubes

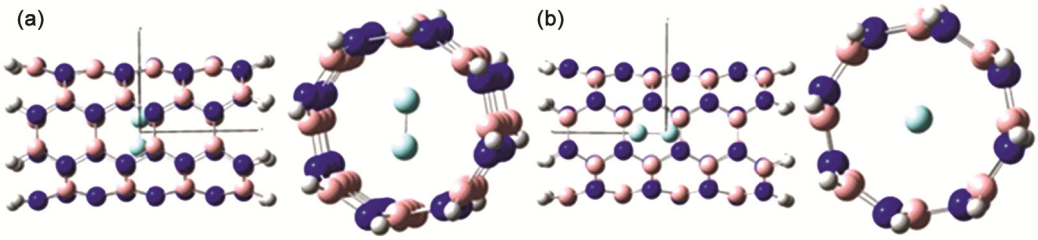

Fig. 1 — (a) Perpendicular and (b) parallel orientation of X_2 inside a BNNT

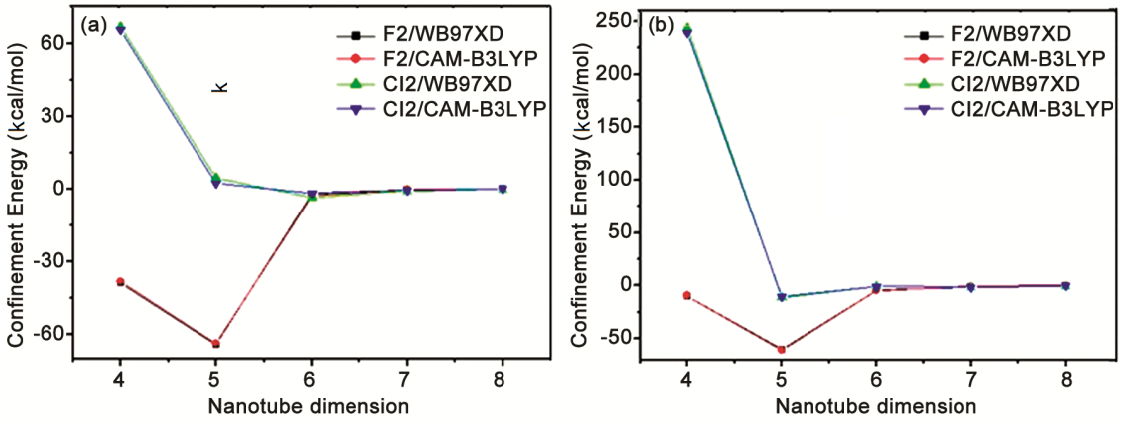

Fig. 2 — Variation of confinement energy of F_2 and Cl_2 versus the diameter of the BNNT for (a) parallel orientation and (b) perpendicular orientation

Table 1 — Confinement energy (kcal/mol) values of F_2 and Cl_2 versus the BNNT diameter calculated with WB97XD and CAM-B3LYP functionals and 6-31G(d,p) basis set

BNNT		F_2@BNNT				Cl_2@BNNT			
		WB97XD		CAM-B3LYP		WB97XD		CAM-B3LYP	
Type	D(Å)	//	⊥	//	⊥	//	⊥	//	⊥
(4,4)	5.83	-38.95	-10.12	-38.21	-9.42	66,84	244.20	65.44	239.82
(5,5)	6.99	-64.20	-60.40	-63.90	-61.30	4,52	-11.45	2.29	-10.30
(6,6)	8.33	-2.06	-4.42	-2.88	-4.73	-3,45	-0.96	-1.81	-0.74
(7,7)	9.79	-0.29	-0.98	-0.23	-0.72	-0,90	-1.48	-0.64	-1.57
(8,8)	11.09	-0.1	-0.42	-0.03	0.32	-0,16	-0.96	-0.09	-0.47

lead to the formation of very stable complexes, compared to the Cl_2@BNNT system. In fact, the confinement energy was negative for F_2 in both orientations for the BNNTs of all dimensions. Notably, for the BNNT with (4,4) dimensions, the confinement energy obtained with the WB97XD and CAM-B3LYP functionals were –38.95 kcal mol^{-1} and –38.21 kcal mol^{-1}, respectively. The confinement energy declined further for fluorine in the BNNT with larger dimensions, i.e., (5,5). Notably, the (5,5) BNNT provided greater stability to the confined F_2. Increasing the dimensions of the BNNT to (6,6), (7,7), and (8,8) did not have a significant effect on the confinement of the F_2 molecule. The energy tended toward zero for these dimensions.

Analysis of Cl_2, produced quite different results from those of F_2. In fact, it was noted that Cl_2 forms less stable complexes compared to F_2, and Cl_2 cannot be confined in the (4,4) BNNT. The stability of the complex formed in the (5,5) BNNT is determined by the confinement orientation. Nevertheless, in the perpendicular position, confinement leads to more stable complexes than in the parallel position.

We have calculated the BSSE corrections to obtain the corrected interaction energies. All the calculated values are listed in Table 2.

We notice that the contribution of BSSE corrections is negligible when the confinement energy is high (in absolute value, for nanotubes (4,4), (5,5) and (6,6)) but increase strongly when the confinement energy is very low (nanotubes (7,7) and (8,8)).

Detection of a negative confinement energy for the dihalide molecule in the nanotubes of different dimensions is the first indicator of interaction between the enclosed molecule and the BNNT nanotube. The absence of negative values of confinement energy attests to the absence or weakness of interactions. To understand the origin of the interactions between the trapped molecule and the walls of the nanotubes, we were interested in the analysis of the structural modifications generated by the confinement process.

Intramolecular X–X distance (X=F or Cl)

The changes in the intramolecular X–X distance (X=F or Cl) for the halides confined in the BNNTs of various dimensions are given in Table 3. Those results show that the variation in the distance depends on the diameter of the nanotubes, the confined molecule (F_2 or Cl_2), and the orientation of the X_2 molecule. The obtained results with the two functional were similar and we report only the results obtained with CAM-B3LYP. The bond length of isolated F_2 molecule determined using CAM-B3LYP/6-31G(d,p) was 1.388 Å, and that of isolated Cl_2 was 1.975 Å. Both values are lower than the experimental values of 1.412 Å[41] and 1.988 Å[41] for F_2 and Cl_2, respectively.

The results in Table 3 show that the equilibrium distance (X-X) did not differ significantly within the large nanotubes, i.e., (6,6), (7,7), and (8,8), for both orientations. This result was predictable because the X_2 molecule (X= F or Cl) is a small molecule placed inside a large hollow space. However, two different phenomena were observed inside the smallest nanotube (4,4) depending on the orientation of the F_2 or Cl_2 molecule. Along the nanotube axis, the X-X bond length did not vary greatly from the equilibrium distance of the isolated molecule.

The second phenomenon indicates that the action of the two molecules F_2 and Cl_2 is different in the perpendicular position. Indeed, we note that in the case of F_2, the F–F distance increased from 1.388 Å for the isolated state to 1.423 Å in F_2@(4,4). However, in the case of Cl_2, the interatomic distance decreased. The Cl-Cl bond length in the (4,4) nanotube was shorter than the equilibrium bond length of the isolated molecule.We will interpret this in what follows in us the values of the atomic or / and van der Waals radii of atoms X and B. To better understand the interaction zones, we calculated the

Table 2 — Basis set superposition error (BSSE) (kcal/mol) values of F_2 and Cl_2 versus the BNNT diameter calculated with CAM-B3LYP functional and 6-31G(d,p) basis set

BNNT		F_2@BNNT		Cl_2@BNNT	
Type	D(Å)	(//)	(⊥)	(//)	(⊥)
(4,4)	5.83	0.0	0.1	0.03	0.05
(5,5)	6.99	0.0	0.0	0.11	0.13
(6,6)	8.33	0.0	0.0	0.0	0.06
(7,7)	9.79	0.08	0.08	0.03	0.04
(8,8)	11.09	0.14	0.29	0.06	0.11

Table 3 — Inter-nuclear distance of X-X (X=F or Cl) in BNNTs in the parallel and perpendicular positions calculated at CAM-B3LYP/6-31G(d,p) level. The experimental values are 1.412Å[(Ref.41)] and 1.988Å[(Ref.41)] for $F_2$and Cl_2, respectively

BNNT		F_2@BNNT		Cl_2@BNNT	
Type	D(Å)	//	⊥	//	⊥
(4,4)	5.83	1.393	1.423	1.990	1.775
(5,5)	6.99	1.394	1.400	2.018	1.942
(6,6)	8.33	1.389	1.390	2.017	2.016
(7,7)	9.79	1.388	1.388	2.018	2.019
(8,8)	11.09	1.388	1.387	2.018	2.018
X_2 Free		1.388		1.975	

changes indicated in Table 4 for the halides in the nanotubes of each diameter[16,17]. The calculated values of those descriptors are compiled in Table 5.

For BNNT with (4,4) dimensions with F_2 in parallel position, the van der Waals radius of F_2 overlaps with that of boron, indicating a strong interaction. The two radii undergo mutual interference; in this case, there is a slight attraction between boron, nitrogen and F_2. This leads to slight elongation of the bond between the two atoms of F_2 to 1.393Å (Fig. 3).

For the nanotube with (4,4) dimension containing the halide in the perpendicular position, the atomic radius of F_2 overlaps with that of boron, where the two radii are within the distance of interference; in this case, there is an attraction between boron, nitrogen and F_2, which leads to elongation of the F–F bond to 1.423 Å (Fig. 3).

For the BNNT with (4,4) dimension with halide in the parallel position, the atomic radius of chlorine is strongly perturbed by the van der Waals radius of boron. The two radii experience mutual interference; in this case, there is an interaction between boron, nitrogen and chlorine, which leads to shortening of the bond between two chlorine atoms to 1.99 Å. In the perpendicular position, the atomic radius of chlorine is very strongly perturbed by the van der Waals radius of boron. The two radii experience mutual interference at a distance of (R8= –5.21 Å); in this case, there is a strong interaction between boron, nitrogen, and chlorine, which leads to extreme shortening of the Cl–Cl bond to 1.775 Å. Chlorine does not fit in the (4,4) BNNT because the molecule is too large and there will be strong van der Waal interactions between the molecules, which explains the high energy found during the confinement of Cl_2

Table 4 — Definition of the descriptors[16,17] R_k (k=1,8) of F_2@BNNT and Cl_2@BNNT complexes in parallel and perpendicular positions. Di represents the diameter of a BNNT

Parallel orientation	Perpendicular orientation	Type of interaction
$R1= D_i-(2R_{atm}(X)+2R_{atm}(B))$	$R5= D_i-(4R_{atm}(X)+2R_{atm}(B))$	Chemical bonding
$R2=D_i-(2R_{atm}(X)+2R_{vdW}(B))$	$R6= D_i-(4R_{atm}(X)+2R_{vdW}(B))$	vdW interaction for X
$R3= D_i-(2R_{vdw}(X)+2R_{atm}(B))$	$R7= D_i-(4R_{vdW}(X)+2R_{atm}(B))$	vdW interaction for B
$R4= D_i-(2R_{vdw}(X)+2R_{vdW}(B))$	$R8= D_i-(4R_{vdW}(X)+2R_{vdW}(B))$	Mutual vdW

Table 5 — The R_k descriptors[16,17] values of the F_2@BNNT and Cl_2@BNNT complexes, in parallel and perpendicular positions

	Dimension	Parallel orientation				Perpendicular orientation			
		R1	R2	R3	R4	R5	R6	R7	R8
F_2@BNNT	(4,4)	3.09	0.99	1.39	-0.71	2.09	-0.01	-1.31	-3.41
	(5,5)	4.25	2.15	2.55	0.45	3.25	1.15	-0.15	-2.25
	(6,6)	5.59	3.49	3.89	1.79	4.59	2.49	1.19	-0.91
	(7,7)	7.05	4.95	5.35	3.25	6.05	3.95	2.65	0.55
	(8,8)	8.35	6.25	6.65	4.55	7.35	5.25	3.95	1.85
Cl_2@BNNT	(4,4)	2.09	-0.01	0.49	-1.61	0.09	-2.01	-3.11	-5.21
	(5,5)	3.25	1.15	1.65	-0.45	1.25	-0.85	-1.95	-4.05
	(6,6)	4.59	2.49	2.99	0.89	2.59	0.49	-0.61	-2.71
	(7,7)	6.05	3.95	4.45	2.35	4.05	1.95	0.85	-1.25
	(8,8)	7.35	5.25	5.75	3.65	5.35	3.25	2.15	0.05

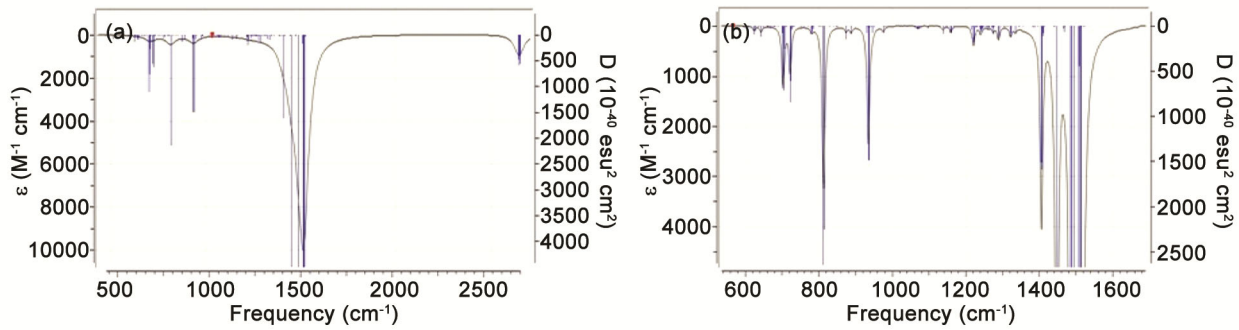

Fig. 3 — Calculated IR spectra at CAMB3LYP/6-31G(d,p) for (a) $F_2(\perp)$@ BNNT and (b) $Cl_2(\perp)$@BNNT (5,5)

inside BNNT with (4,4) dimension, where the energy calculated with WB97XD and CAM-B3LYP functionals were 244.20 kcal mol^{-1} and 239.82 kcal mol^{-1}, respectively (Fig. 3).

For the BNNT with (5,5) dimension, the binding energy for confined difluorine decreased compared to that with (4,4) dimension but remained slightly higher than that of the F-F bond in the free state. Indeed, in the parallel position, the van der Waals radius of fluorine is 0.45 Å from the van der Waals radius of boron. This distance is small, and the interaction does not influence the F–F distance (Table 6).

For the BNNT with (5,5) dimension with F_2 in the perpendicular position, the van der Waals radius of difluorine is perturbed by the radius of the boron; the two radii undergo mutual interference with a distance of (R7= –0.15Å). In this case, there is an attraction between boron, nitrogen, and F_2, which leads to slight elongation of the F–F bond to 1.40 Å. In the case of Cl_2 in the BNNT with (5,5) dimension, the atomic radius of chlorine is slightly perturbed by the van der Waals radius of boron. The two radii experience mutual interference (R4= –0.45 Å). In this case, there is a slight interaction between boron, nitrogen, and chlorine, which leads to relaxation of the bond between the two chlorine atoms, which is lengthened to 2.018 Å. For the BNNT with (5,5) dimension with chlorine in the perpendicular position, the atomic radius of chlorine is strongly perturbed by the van der Waals radius of boron. The two radii mutually interfere at a distance of (R8= –4.05 Å). In this case, there is a strong interaction between boron, nitrogen, and chlorine, which leads to shortening of the Cl–Cl bond to 1.942 Å (Table 6). For the BNNTs with (6,6), (7,7), and (8,8) dimensions, the radii of boron and the halides did not overlap. The halides did not undergo any confinement restriction in the BNNTs with these diameters (Table 6).

Vibration frequency

The isolated X_2 (X=F or Cl) molecule is not IR active because its dipole moment is zero. Confinement of the halides in the nanotubes induces a dipole moment, especially in the BNNTs with small dimensions. In this section, we explore whether this induced dipole moment affects the intensity of the vibration frequencies of X-X (X=F or Cl) bond, as reported for H_2[Ref. 17]. In this work, the normal vibration modes were calculated for the $X_2(\perp)$@BNNT system (X=F or Cl) at the DFT/CAM-B3LYP/6-31G(d,p) level of theory. The results are summarised in Table 7. The vibrational frequencies were scaled by a factor of 0.960461[Ref. 41]. The value of $\nu_{F\text{-}F}$ was 1019 cm^{-1}, which remains close to the values for F_2 confined in the BNNTs with (6,6), (7,7), and (8,8) dimensions. This result shows once again that for the BNNTs with (6,6) dimensions and larger, in the perpendicular position, F_2 is not influenced by the walls of the BNNT nanotubes.

In addition, we note that the vibrational frequency of F_2 in the BNNT with (5,5) dimensions is close to the experimental value of 916.929 cm^{-1}[Ref. 42]. On the other hand, for free Cl_2, the vibrational frequency is approximately 559.751 cm^{-1}[Ref. 42], which remains close to the value for Cl_2 confined in BNNT with (5,5) dimensions in the perpendicular orientation.

The intensity of the vibration of X_2 (X=F or Cl) molecule was almost zero when the halides were confined to the nitrogen boron nanotubes of different dimensions. As in CNTs,[14] the vibrational frequency of X_2@BNNT is not useful for guiding experimenters in the detection of F_2, unlike the case for other molecules such as H_2, where the vibrational frequency of H_2 is a good tool for its detection and for differentiation of the diameters of CNTs[16], BNNTs[16], and GeNTs[17].

The most remarkable result comes from the analysis of the vibration spectra obtained after confinement of the halides in the BNNTs. The data highlight several vibrational modes of the X–X (X=F or Cl) bond like stretching, rocking, wagging, bending, and twisting. The interaction of the X-X molecule with the BNNT will lead to charge transfer and a change in the charge distribution in the X-X molecule, producing a new detectable vibration for the bond stretches. The appearance of these modes depends on the dimensions of the BNNT used.

Indeed, we noted that for the halide confined in BNNT with (4,4) dimensions, there are four modes, namely stretching, rocking, wagging, and twisting. For the halides in the (5,5) BNNT, there are three vibrational modes like stretching, bending, and rocking for each F_2 and Cl_2. For the BNNT with (6,6) dimensions, we find only one mode that corresponds to stretching for F_2 and two modes (stretching and rocking) for Cl_2. In the BNNTs with (7,7) and (8,8) dimensions, two vibrational modes (stretching and twisting) were observed for F_2 and Cl_2. In addition, we note that the energies of the rocking, wagging, bending, and twisting type vibration modes of confined X_2ranged from 16.53 to 288.65 cm^{-1}. These bands are located in a relatively clear area of the

Table 6 — Schematization of van der Waals radius and atomic radius of boron and difluorine F–F and chlorine Cl-Cl within the BNNTs

a

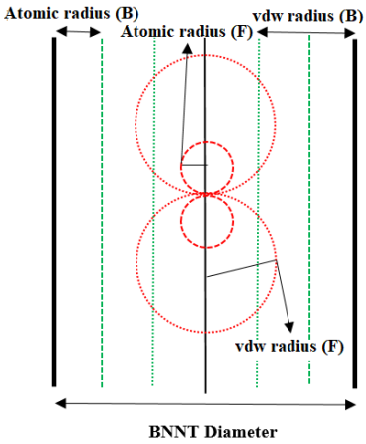

b

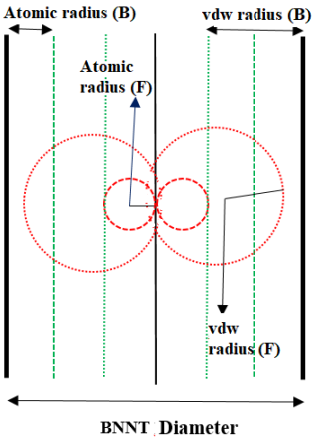

c

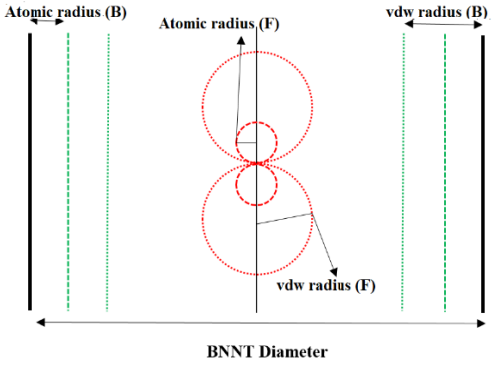

d

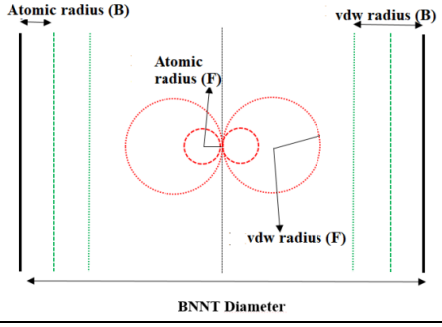

e

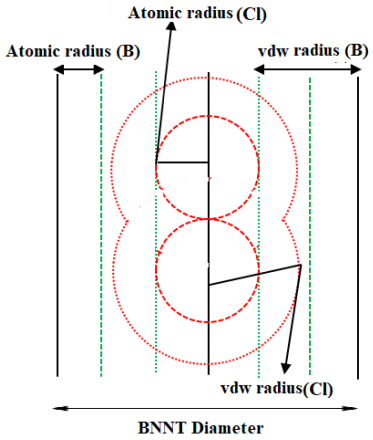

f

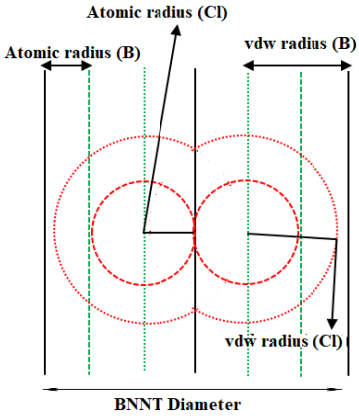

g

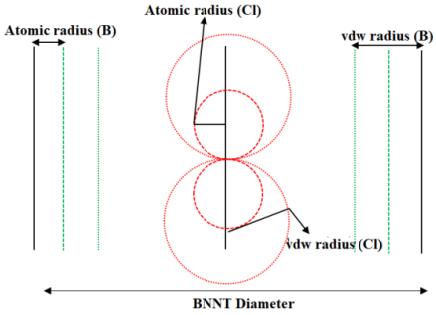

h

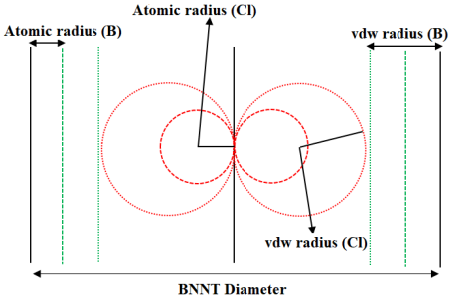

Table 7 — $\nu_{Cl\text{-}Cl}$ and $\nu_{F\text{-}F}$ scaled frequencies (cm^{-1}) values for $X_2(\perp)$@BNNT with (X=F or Cl) at DFT/CAM-B3LYP/6-31G(d,p) level of calculation. Nv designs the number of vibrational modes

		Cl_2			F_2		
(n,n)	Nv	Mode	Frequency	Intensity	Mode	Frequency	Intensity
X_2	1	*Stretching*	532.24	0.0	*Stretching*	1019	0.0
(4,4)	240	*Stretching*	520.67	1.18	*Stretching*	492.41	1.7736
		Rocking	288.65	2.49	*Rocking*	262.49	2.6814
		Wagging	108.77	0.21	*Wagging*	185.91	0.5293
		Twisting	284.68	0.31	*Twisting*	138.50	6.3179
(5,5)	300	*Stretching*	529.70	0.00	*Stretching*	1034.52	1.1637
		Wagging	121.12	0.28	*Bending*	106.40	0.2174
		Twisting	183.37	0.00	*Rocking*	91.09	0.0554
(6,6)	360	*Stretching*	556.05	0.17	*Stretching*	1009.23	0.0004
		Rocking	77.18	0.13			
(7,7)	420	*Stretching*	555.24	0.00	*Stretching*	1017.06	0.0001
		Twisting	16.53	0.00	*Twisting*	41.14	0.0000
(8,8)	530	*Stretching*	553.09	0.00	*Stretching*	1099.85	0.0000
		Twisting	40.27	0.00	*Twisting*	41.49	0.0000

infrared spectrum and can be used to experimentally monitor the process of X_2 confinement in BNNT nanotubes.

Conclusions

DFT calculations were performed to study the interaction between the X_2 (X=F or Cl) molecule and different BNNTs dimensions (4,4), (5,5), (6,6), (7,7) and (8,8) in parallel or perpendicular position along the nanotube axis. The calculations clearly show that compared to Cl_2, F_2 forms a very stable complex with the BNNTs with (4,4) and (5,5) dimensions. The interaction between the X_2 molecule and BNNT nanotube differed according to the dimensions of the confinement space and the molecular orientation. The van der Waals interactions between the X_2 molecule and BNNTs lead to competitive behaviour at the nanometric level, which is influenced by the orientation of the molecule. These interactions will lead to charge transfer and a change in the charge distribution in the X_2 molecule, producing a new detectable vibration for the bond stretches. The appearance of these modes depends on the dimensions of the BNNT used. The intensity of the vibration of the X_2 molecule was almost zero, the vibrational frequency of X_2@BNNT is not useful for guiding researchers in the detection of X_2, unlike the case for other molecules such as H_2.

References

1 Rubio A, Corkill J L & Cohen M L, *Phys Rev B,* 49 (1994) 5081.

2 Chopra N G, Luyken R J, Cherrey K, Crespi V H, Cohen M L, Louie S G & Zettl A, *Science,* 269 (1995) 966.

3 Xiao Y, Yan X H, Cao J X, Ding J W, Mao Y L & Xiang J, *Phys Rev B,* 69 (2004) Article 205415.

4 Golberg D, Bando Y, Kurashima K & Sato T, *Scr Mater,* 44 (2001) 1561.

5 Wang J, Lee C H & Yap Y K, *Nanoscale,* 2 (2010) 202834.

6 Boinovich L B, Emelyanenko A M, Pashinin A S, Lee C H, Drelich J & Yap Y K, *ACS J Surf Colloids,* 28 (2012) 1206.

7 Li L H & Chen Y, *ACS J Surf Colloids,* 26 (2010) 5135.

8 Hernández E, Goze C, Bernier P & Rubio A, *Phys Rev Lett,* 80 (1998) 4502.

9 Chopra N G & Zettl A, *Solid State Commun,* 105 (1998) 297.

10 Zhi C, Bando Y, Tang C, Xie R, Sekiguchi T & Golberg D, *J Am Chem Soc,*127 (2005) 15996.

11 Chen Y, Zou J, Campbell S J & Le Caer G, *Phys Lett,* 84 (2004) 2430.

12 Tang C, Bando Y, Ding X, Qi S & Golberg D, *J Am Chem Soc,* 124 (2002) 14550.

13 Ma R, Bando Y, Zhu H, Sato T, Xu C & Wu D, *J Am Chem Soc,* 124 (2002) 7672.

14 Gao Z, Zhi C, Bando Y, Golberg D & Serizawa T, *Nanobiomedicine,* 1 (2014) 7.

15 Ganji M D & Mirzaei S, *Procedia Materials Science,* 11 (2015) 403.

16 Gtari W F & Tangour B, *Int J Quantum Chem,* 113 (2013) 2397.

17 Belmiloud Y, Djitli W, Abdeldjebar H, Abdelatif M L, Tangour B & Brahimi M, *Superlattices Microstruct,* 101 (2017) 547.

18 Djitli W, Abdelatif M L, Belmiloud Y, Abdeldjebar H, Brahimi M & Tangour B, *Superlattices Microstruct,* 122 (2018) 596.

19 Wang L, Zhao J, Li F, Fang H & Lu J P, *J Phys Chem C,* 113 (2009) 5368.

20 Chaban V V & Prezhdo O V, *ACS Nano,* 5 (2011) 5647.

21 Gannouni A, Ouraghi M, Boughdiri S, Bessrour R, Benaboura A & Tangour B, *J Comput Theor Nanosci,* 9 (2012) 379.

22 Dargouthi S, Boughdiri S & Tangour B, *Actachimica Slovenica,* 62 (2015) 445.

23 Bessrour R, Belmiloud Y, Hosni Z & Tangour B, *AIP Conf Proc*, 1456 (2012) 229.

24 Golberg D, Bando Y, Huang Y, Terao T, Mitome M Tang Cet & Zhi C, *ACS Nano,* 4 (2010) 2979.

25 Opalovsky A A, Fedorov V E & Fedotova T D, *J Therm Anal Calorim,* 1 (1969) 301.
26 Hattori Y & Touhara H, *New Fluorinated Carbons: Fundamentals and Applications*, (Elsevier), 2017, pp. 113.
27 Hattori Y, Kanoh H, Okino F, Touhara H, Kasuya D, Yudasaka M, Iijima S & Kaneko K, *J Phys Chem B,* 108 (2004) 9614.
28 Adamska M & Narkiewicz U A, *J Fluor Chem,* 200 (2017) 179.
29 Lokhandwala K A, Segelke S, Nguyen P, Baker R W, Su T T & Pinnau I, *Chem Res,* 38 (1999) 3606.
30 Felah Gtari W & Tangour B, *Can. J. Chem,* 94 (2016) 15.
31 Bordiga S, Turnes Palomino G, Pazè C & Zecchina A, *Microporous Mesoporous Mater,* 34 (2000) 67.
32 Corbin D R, Abrams L, Jones G A, Smith M L, Dybowski C R, Hriljac J A & Parise J B, *J Chem Soc, Chem Commun,* 12 (1993) 1027.
33 Han W-Q & Zettl A, *J Am Chem Soc,* 125 (2003) 2062.
34 Newark D E: University of Delaware.*TubeGen*, 2011.
35 Chai J-D & Head-Gordon M, *Phys Chem Chem Phys,* 10 (2008) 6615.
36 Chai J-D Head-Gordon M, *J Chem Phys*, 128 (2008) 84106. DOI: 10.1039/B810189B.
37 Yanai T, Tew D P & Handy N C, *Chem Phys Lett,* 393 (2004) 51.
38 *GAUSSIAN 09 Wallingford CT*; Gaussian, Inc, 2009.
39 Simon S, Duran M & Dannenberg J J, *J Chem Phys,* 105 (1996) 11024–11031.
40 Boys S F & Bernardi F, *Mol Phys,* 19 (1970) 553.
41 Huber K P & Herzberg G, (*MA: Springer US*), 1979.
42 Irikura K K, *J Phys Chem Ref Data,* 36 (2007) 389.